Pis'ma v ZhETF, vol. 100, iss. 2, pp. 134 – 140

Multigap superconductivity in doped *p*-type cuprates

Ya. G. Ponomarev[+1)], *V. A. Alyoshin*[*], *E. V. Antipov*[*], *T. E. Oskina*[*], *A. Krapf*[×], *S. V. Kulbachinskii*[+°], *M. G. Mikheev*[+], *M. V. Sudakova*[+], *S. N. Tchesnokov*[+], *L. M. Fisher*[°]

[+]*Faculty of Physics, Lomonosov MSU, 119991 Moscow, Russia*

[*] *Department of Chemistry, Lomonosov MSU, 119991 Moscow, Russia*

[×]*Institut fur Physik, Humboldt-Universität zu Berlin, D-12489 Berlin, Germany*

[°]*Lenin Russian Electrotechnical Institute, 111250 Moscow, Russia*

Submitted 29 May 2014

Andreev and tunneling spectroscopy studies of $Bi_2Sr_2Ca_{n-1}Cu_nO_{2n+4+\delta}$, $HgBa_2Ca_{n-1}Cu_nO_{2n+2+\delta}$ and $Tl_2Ba_2Ca_{n-1}Cu_nO_{2n+4+\delta}$ have shown that superconductivity in single-layer ($n = 1$) and two-layer ($n = 2$) phases has a single-gap character. Qualitatively different results were obtained for three-layer phases. In doped *p*-type Hg-1223, Bi-2223, and Tl-2223 samples two (or three) superconducting gaps were observed. The existence of multigap superconductivity in superconducting cuprates with $n \geq 3$ is explained by a difference in doping levels of outer (OP) and internal (IP) CuO_2-planes.

DOI: 10.7868/S0370274X14140112

1. Introduction. It has been found that the layered cuprate superconductors $Bi_2Sr_2Ca_{n-1}Cu_nO_{2n+4+\delta}$, $HgBa_2Ca_{n-1}Cu_nO_{2n+2+\delta}$, and $Tl_2Ba_2Ca_{n-1}Cu_nO_{2n+4+\delta}$ are natural superlattices of the type SISI... where S – superconducting blocks containing one or more of CuO_2-planes intercalated with calcium, I – insulating blocks (spacers) having a standard structure for a given cuprate family. Introduction of the excess oxygen O_δ in the central part of spacers plays a key role in the formation of superconducting properties of CuO_2-blocks [1]. Within one superconducting phase with a predetermined number n of CuO_2-planes the maximum superconducting transition temperature $T_{c\,\max}$ can be reached by selecting a proper concentration of excess oxygen O_δ. Note that when $\delta = 0$ the above-mentioned compounds are Mott insulators with antiferromagnetic ordering of spins in CuO_2-planes. Excess oxygen binds electrons from CuO_2-layers, generating in them *p*-type charge carriers. A weak oxygen doping destroys the long-range antiferromagnetic order, causing a dielectric-to-metal transition. As a result an open hole Fermi surface is formed [1] with the Fermi level in the vicinity of an extended van Hove singularity (EVHS) with giant peaks in the quasiparticle density of states [2].

It is very important that the oxygen O_δ does not create strong scattering centers in CuO_2-blocks, as it is located at a considerable distance from them. At the same time, the excess oxygen forms charge traps in the center of spacers, creating favorable conditions for resonant tunneling in the *c*-direction [1]. At $T < T_c$ doped HTSC crystals behave like a stack of strongly coupled Josephson junctions and the superconducting current in the *c*-direction, therefore, has a Josephson nature (weak superconductivity).

High-temperature superconductivity is realized in the CuO_2-planes within a relatively narrow range of concentrations of impurity holes p. According to the photoemission spectroscopy a superconducting gap is maximal in Γ–M direction and minimal in Γ–Y direction [1, 2]. Anisotropy of the gap decreases significantly with increasing p [3].

Note that there is a possibility of the Fermi level pinning at the EVHS in a certain range of concentrations of impurity holes p. The critical temperature T_c changes with p by a parabolic law [4] and there is a scaling of the critical temperature T_c and superconducting gap Δ on doping [5].

According to Abrikosov a high critical temperature T_c in HTSC is realized mainly due to the presence of EVHS near the Fermi level [1, 2]. EVHS has been observed experimentally in cuprate superconductors by photoemission and tunneling spectroscopies [2, 5, 6]. In Abrikosov model a major role in the formation of the pairing potential is played by virtual optical phonons with small wave vectors $\mathbf{k}$. Due to these phonons pairing carriers are kept in the vicinity of the EVHS ("forward" scattering). Abrikosov has shown that near op-

[1)]e-mail: ponomarevy@mail.ru

timal doping a pre-exponential factor in the expression for T_c loses the Debye frequency causing a disappearance of the isotope effect. With departure from the optimal doping the Debye frequency reappears in the pre-exponential factor, and the isotope effect is restored. The latter corresponds to the experimental data.

In superconducting cuprates $HgBa_2Ca_{n-1}Cu_nO_{2n+2+\delta}$ (HBCCO), $Bi_2Sr_2Ca_{n-1}Cu_nO_{2n+4+\delta}$ (BSCCO), and $Tl_2Ba_2Ca_{n-1}Cu_nO_{2n+4+\delta}$ (TBCCO) phases Hg-1201, Bi-2201, and Tl-2201 contain a single CuO_2-plane, phases Hg-1212, Bi-2212, and Tl-2212 contain two CuO_2-planes and phases Hg-1223, Bi-2223, and Tl-2223 – three CuO_2-planes. In HBCCO, BSCCO, and TBCCO superconducting CuO_2-blocks are separated by insulating structural blocks (spacers) BaO–HgO_δ–BaO, SrO–BiO–BiO–SrO, and BaO–TlO–TlO–BaO respectively.

The problem of obtaining optimally doped cuprate samples with $n \geq 3$ by a standard method becomes complicated. For example, NMR-spectroscopy studies [7] showed that a copper nuclear magnetic resonance in $HgBa_2Ca_{n-1}Cu_nO_{2n+2+\delta}$ with $n \geq 3$ transforms into a doublet which was explained by different levels of oxygen doping in internal (IP) and outer (OP) CuO_2-planes. This effect explains a non-trivial dependence of the critical temperature on the number n of CuO_2-planes [8]. It is obvious that the appearance of defects in superconducting CuO_2-planes will primarily cause smearing of the EVHS and, consequently, suppression of superconductivity. To maximize the critical temperature $T_{c\,\max}$ it is necessary to fulfill two conditions: i) the Fermi level should be aligned with the EVHS (using doping), ii) the structural perfection of CuO_2-planes must be provided. Both of these conditions are fulfilled automatically when HTSC are doped with excess oxygen, which changes the concentration of holes in CuO_2-plane being out of the plane (in the central part of the insulating blocks). It is extremely important that the excess oxygen has practically no effect on the mobility of impurity holes in superconducting CuO_2-planes.

The results obtained in the present investigation are as follows: 1) the Andreev and tunneling spectroscopy studies showed that superconductivity in the optimally doped samples of Bi-2201 ($T_c = 25 \pm 3$ K), Hg-1201 ($T_c = 93 \pm 2$ K), Bi-2212 ($T_c = 92 \pm 2$ K), Tl-2212 ($T_c = 105 \pm 2$ K), and Hg-1212 ($T_c = 120 \pm 5$ K) has a single-gap character; 2) superconductivity in Bi-2223 ($T_c = 110 \pm 5$ K), Tl-2223 ($T_c = 118 \pm 5$ K), and Hg-1223 ($T_c = 124 \pm 5$ K) has a multigap character due to the difference in doping levels of internal (IP) and outer (OP) CuO_2-planes in superconducting blocks.

2. The experimental procedure and the samples studied. The measuring system is assembled on the basis of multifunctional input-output board AT-MIO-16X (National Instruments) and a personal computer. Temperature dependences of a sample resistance $R(T)$, current-voltage characteristics $I(V)$, and differential conductivity $dI(V)/dV$ of break-junctions were measured using a four-probe technique. Current-voltage characteristics (CVCs) were recorded by a fixed current method. Temperature control was carried out using a calibrated Ge sensor. $dI(V)/dV$-characteristics were recorded using a high speed high precision automatic digital AC bridge (modulation method).

Polycrystalline $HgBa_2Ca_{n-1}Cu_nO_{2n+2+\delta}$ tablets with $n = 1$, 2, and 3 were synthesized at the Department of Chemistry, Moscow State University [9, 10]. Single crystals and polycrystalline samples of $Bi_2Sr_2Ca_{n-1}Cu_nO_{2n+4+\delta}$ were synthesized at the Humboldt University (Berlin) and Moscow State University [11, 12]. Tablets were cut into samples of rectangular form ($0.3 \times 0.7 \times 2.0\,\text{mm}^3$) using the MTI diamond wire saw. Samples were then mounted on a substrate made of copper foil coated laminate. The copper foil was cut into four rectangular plates serving as electrical contact pads. A short groove was made in the foil substrate relatively deep and served as a stress concentrator. Low-resistance contacts between the sample and the current and potential leads were prepared using indium-gallium solder. At room temperature the solder is in a liquid phase which prevents samples from being damaged due to inevitable deformations of the substrate during installation. After cooling the In–Ga solder firmly fixes sample in a proper position. The substrate for the sample was glued to beryllium copper spring of thickness 0.3 mm. When gently pressing on the back side of the spring with a micrometer screw caliper, the sample was broken just above the stress concentrator. Generation of a crack in the sample (along *ab*-planes mainly) and subsequent adjustment of the contact was made in liquid helium.

3. Experiment results. The obvious advantages of the technique used for junction preparation in HTSC samples (break junction technique) include a high surface quality of cryogenic cleavages (both in single crystals and polycrystalline samples) and a possibility of tuning of point contacts with a micrometer screw. It should be also noted that the defects are usually ejected to the grain boundaries in the process of synthesis. For this reason it is impossible to obtain ballistic (Sharvin) point contacts utilizing **cracks between** the grains. In the present investigation all point contacts in the ballis-

tic regime were formed using cryogenic **intragranular** cleavages.

The point-contact (Andreev) spectroscopy gives, in principle, more precise values of the superconducting gap Δ than the tunneling spectroscopy. First, the subharmonic gap structure (SGS) in the CVCs of the contacts due to multiple Andreev reflections (MAR) becomes detectable only in the case of submicron size of these contacts and, as a consequence, the heterogeneity of the samples appears to be less pronounced. Second, the gap parameter is calculated from a series of Andreev singularities, the number n of which in clean contacts can be five to seven, what significantly improves the accuracy of the calculations. During formation of a contact the cracks develop along ab-planes due to the layered structure of cuprates. Thus the transport current in nanocontacts is parallel to the c-axis in most cases.

The main features of the current-voltage characteristics (CVCs) of ScS-type Andreev contacts include a large excess current at low bias voltages and subharmonic gap structure (SGS), comprising a series of sharp dips of dynamic conductance dI/dV at voltages that satisfy the condition [13]:

$$V_n = 2\Delta/en, \qquad (1)$$

where $n = 1, 2, \ldots$.

Usually, the SGS is associated with MAR in ScS ballistic Sharvin nanocontacts [13, 14]. This type of structure has to be distinguished from the SGS in the CVCs of quantum point contacts with a low transparency interface [15]. In the latter case, the SGS consists of a series of **maxima** of the dynamic conductivity at voltages $V_n = 2\Delta/en$. With increasing interface transparency a series of **maxima** turns into a series of **minima**, which coincides with the results of Kummel et al. [14] for clean classical SNS contacts. We assume that the theoretical model of Kummel is applicable to our junctions. Anisotropy of the gap in ab-plane (d-wave symmetry) causes smearing of SGS. The position of singularities in this case is determined by the value of the **maximal gap** $\Delta_{\max}$ [16].

Quality of SGS is strongly dependent on the ratio of the quasiparticle mean free path l to the contact radius a [14]. In the ballistic regime ($l \gg a$) the normal resistance R of a Sharvin contact is [17]:

$$R = (4/3\pi)(\rho l/a^2), \qquad (2)$$

where ρ is a metal volume resistivity.

For mercury cuprates, for example, $\rho l \approx 1 \times 10^{-9}\,\Omega\cdot\mathrm{cm}^2$ and $l \approx 3 \cdot 10^{-6}$ cm [18, 19]. Equation (2) can be used for a rough estimation of a contact radius a. A typical normal resistance R of our contacts at $T = 4.2$ K is in the range: 10–30 Ω. From this we can estimate the radius of our point contacts: $a \approx 2 \cdot 10^{-6}$ cm. So for our contacts: $l \approx a$, which is in agreement with a limited number n of Andreev singularities that make SGS [14]. The above estimation is roughly true also for BSCCO and TBCCO nanocontacts.

We have found that CVCs of Andreev junctions in doped Hg-1201, Hg-1212, Bi-2201, Bi-2212, and Tl-2212 demonstrate SGS typical for **single-gap** superconductivity (Figs. 1–5). Values of the gaps obtained from Andreev spectroscopy and tunneling spectroscopy coincide within experimental errors (Fig. 4).

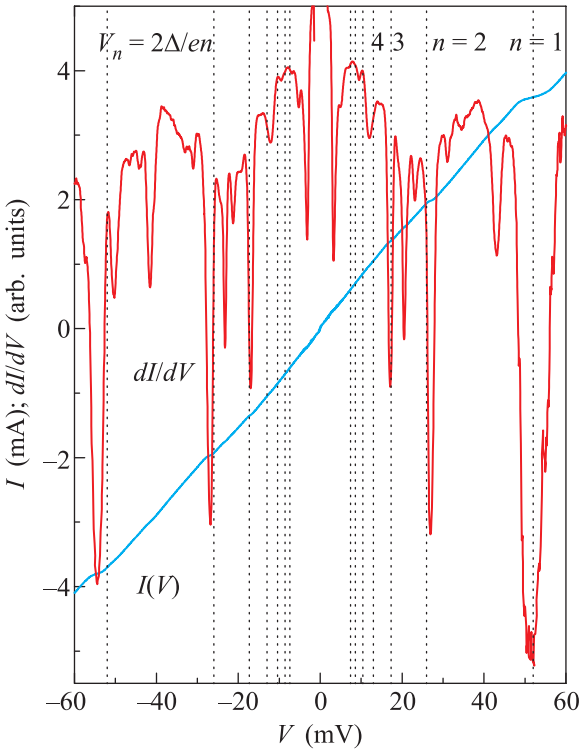

Fig. 1. $I(V)$- and dI/dV-curves for Andreev ScS nanocontact in optimally doped Hg-1201 (sample AN1D11, $T = 4.2$ K, $T_c = 94$ K, $\Delta = 26$ meV, $2\Delta/kT_c = 6.4$). Vertical dashed lines correspond to expected positions of Andreev singularities $V_n = 2\Delta/en$

In the case of three-layered cuprates Hg-1223, Bi-2223, and Tl-2223 [20] the situation changed in a qualitative way (Figs. 6 and 7 and Tables 1–3). In the CVCs of Sharvin-type Hg-1223, Bi-2223, and Tl-2223 nanocontacts there are two (or three) independent subharmonic gap structures corresponding to substantially different in magnitude superconducting gaps (Figs. 6 and 7 and Table 3 [20]).

4. Discussion. As we have noted above, all studied junctions in Hg-1201, Hg-1212, Hg-1223, Bi-2201, Bi-

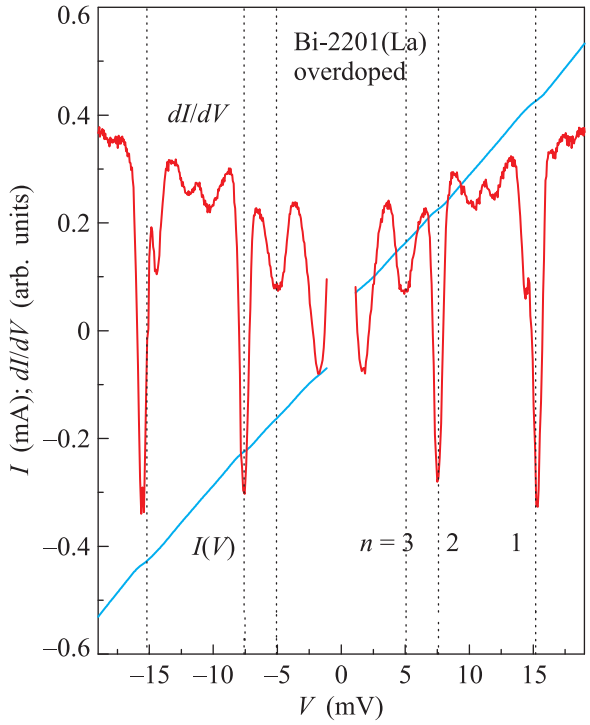

Fig. 2. $I(V)$- and dI/dV-curves for Andreev ScS nanocontact in overdoped Bi-2201 (sample K3D, $T = 4.2$ K, $T_c = 17 \pm 0.5$ K, $\Delta = 7.6 \pm 0.3$ meV, $2\Delta/kT_c = 10.4 \pm 1$). Vertical dashed lines correspond to expected positions of Andreev singularities $V_n = 2\Delta/en$

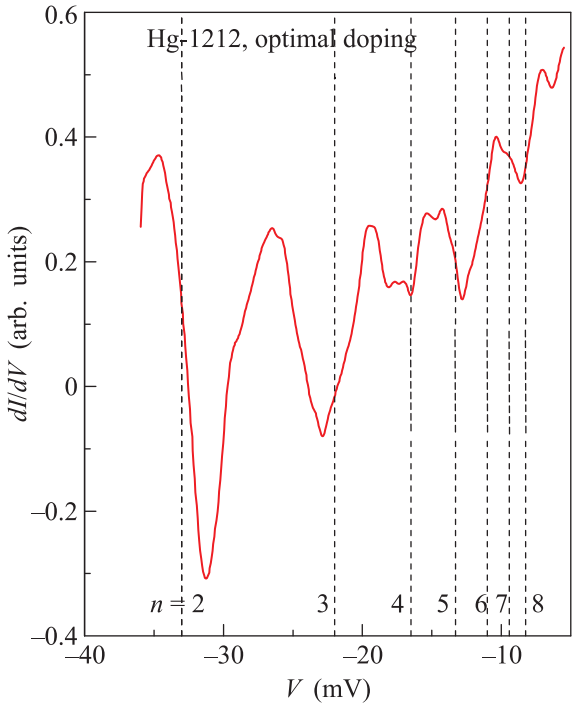

Fig. 3. dI/dV-curve for Andreev ScS nanocontact in optimally doped Hg-1212 ($T = 4.2$ K, $T_c = 120 \pm 5$ K, $\Delta = 33$ meV, $2\Delta/kT_c = 6.4$). Vertical dashed lines correspond to expected positions of Andreev singularities $V_n = 2\Delta/en$

2212, Bi-2223, Tl-2212, and Tl-2223 [20] should be considered to be the ballistic type nanocontacts of Sharvin type (Figs. 1–7). The CVC's of the most clean contacts of this kind contain up to 5–7 Andreev singularities. For single-gap superconductors (Figs. 1–5) the gap magnitude can be determined with sufficient accuracy from linear dependences $V_n(1/n)$ (Tables 1–3). The results of the present investigation for single-layer ($n = 1$) and two-layer ($n = 2$) cuprates are in good agreement with data of other authors (see, for example, [21] and Table 1). Due to the layered structure of cuprates the transport current through nanosteps on the surface of cryogenic cleaves is directed mainly along c-axis. For both tunneling and Andreev regimes the maximal value of the gap $\Delta_{\max}$ was measured (Fig. 4).

For phases with $n \geq 3$ we have two (or three) SGS's and, consequently, two (or three) dependences $V_n(1/n)$ (Tables 1–3). The explanation of this phenomenon can be found in publications [7, 8], where authors had taken into account the specificity of doping of multilayered HTSC. According to the model proposed in [7, 8], the doping level of internal CuO_2-planes in the superconducting block is always lower than the doping level of the outer CuO_2-planes. This is caused by the strong screen-

Table 1

Superconducting parameters of $HgBa_2Ca_{n-1}Cu_nO_{2n+2+\delta}$ ($n = 1, 2, 3$), estimated in the present investigation. For comparison the data of publications [21, 22] are presented

Sample	T_c, K	Δ, meV	$2\Delta/kT_c$	Source
Hg-1201, polycrystalline samples				
AN1D11	94	26	6.4	Pres. inv.
HG1201	93	26	6.5	[21]
Hg-1212, polycrystalline samples				
PCD01A	120	33	6.4	Pres. inv.
Hg-1223, polycrystalline samples				
A52D10	124	$\Delta_{OP} =$ $= 49$ meV; $\Delta_{IP} =$ $= 12$ meV	$\frac{2\Delta_{OP}}{kT_c} = 9.2$ $\frac{2\Delta_{IP}}{kT_c} = 2.25$	Pres. inv.
HG1223	132	$\Delta_{OP} =$ 37.8 meV; $\Delta_{IP} =$ $= 55.9$ meV	$\frac{2\Delta_{OP}}{kT_c} = 6.6$ $\frac{2\Delta_{IP}}{kT_c} = 9.8$	[22]

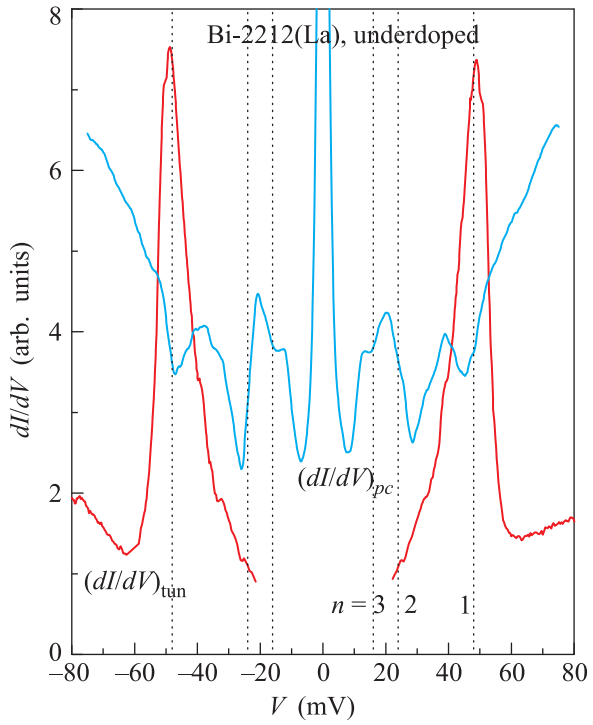

Fig. 4. (Color online) dI/dV-curves for nanocontact in Andreev regime (blue line) and tunneling regime (red line) in underdoped Bi-2212 (sample K3, $T = 4.2$ K, $T_c = 78 \pm 2$ K, $\Delta = 24 \pm 0.5$ meV, $2\Delta/kT_c = 7.1 \pm 0.4$). Vertical dashed lines correspond to expected positions of Andreev singularities $V_n = 2\Delta/en$

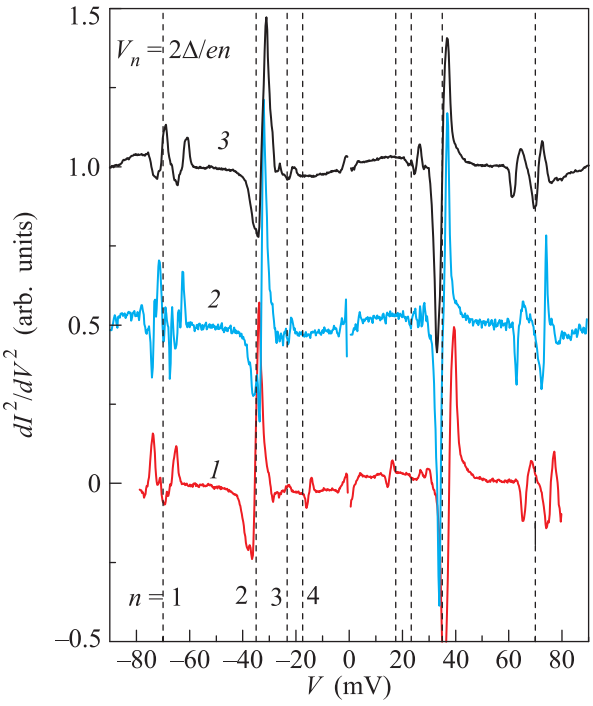

Fig. 5. d^2I/dV^2-curves for Andreev ScS contacts in optimally doped Tl-2212 ($T = 4.2$ K, $T_c = 105$ K, $\Delta = 35$ meV, $2\Delta/kT_c = 7.7$). Curves *1*, *2*, and *3* were plotted after successive readjustments of the contact

Table 2

Superconducting parameters of $Bi_2Sr_2Ca_{n-1}Cu_nO_{2n+4+\delta}$ ($n = 1, 2, 3$), estimated in the present investigation

Sample	T_c, K	Δ, meV	$2\Delta/kT_c$	Source
Bi-2201, single crystals				
K3D, overdoped	17	7.6	10.4	Pres. inv.
Bi-2212, single crystals				
KA3A, underdoped	78	24	7.1	Pres. inv.
Bi2223, polycrystalline samples				
TEO2, underdoped	104	$\Delta_{OP} =$ $= 42$ meV $\Delta_{IP} =$ $= 5.7$ meV	$\frac{2\Delta_{OP}}{kT_c} = 9.4$ $\frac{2\Delta_{IP}}{kT_c} = 1.3$	Pres. inv.

Table 3

Superconducting parameters of $Tl_2Ba_2Ca_{n-1}Cu_nO_{2n+4+\delta}$ ($n = 2, 3$), estimated in the present investigation

Sample	T_c, K	Δ, meV	$2\Delta/kT_c$	source
Tl-2212, polycrystalline sample				
Optimally doped	105	35	7.7	Pres. inv.
Tl-2223, polycrystalline sample				
Optimally doped	118	$\Delta_{OP1} =$ 50 meV; $\Delta_{OP2} =$ $= 45$ meV; $\Delta_{IP} =$ $= 5.5$ meV	$\frac{2\Delta_{OP1}}{kT_c} = 9.8$ $\frac{2\Delta_{OP2}}{kT_c} = 8.8$ $\frac{2\Delta_{IP}}{kT_c} = 1.1$	Pres. inv.

ing of the internal CuO_2-planes by the outer planes, which are metallized by doping (due to insulator-metal transition). It is for this reason that the NMR resonance at the copper nuclei is transformed into a doublet [7].

A significant difference in doping levels of outer and internal CuO_2-planes in the superconducting blocks originated a scenario of coexistence of antiferromagnetism and superconductivity in high-T_c superconductors.

It should be mentioned that for a three-layer phase there is a discrepancy in assignment of the values of the gaps to internal and outer CuO_2-planes in the present investigation and work [22]. It follows from [5, 6] that

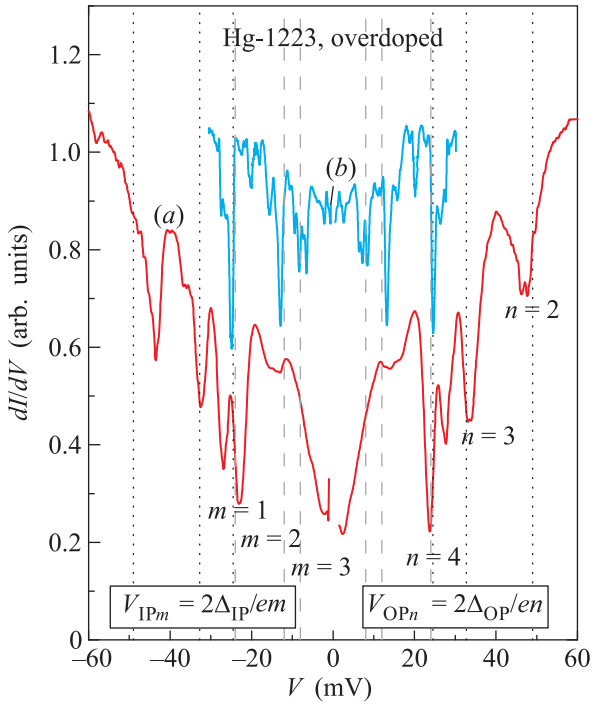

Fig. 6. dI/dV-curves for nanocontacts in Andreev regime in overdoped three-layer Hg-1223 ($T = 4.2$ K, $T_c = 124 \pm 5$ K, $\Delta_{OP} = 49$ meV, $\Delta_{IP} = 12$ meV, $2\Delta_{OP}/kT_c = 9.2$, $2\Delta_{IP}/kT_c = 2.25$). (a) – dI/dV-curve with two SGSs, corresponding to large Δ_{OP} and small Δ_{IP} gaps. (b) – A fragment of dI/dV-curve after readjustment of the contact. SGS corresponds to a small gap Δ_{IP}. Vertical dashed lines mark the expected positions of Andreev singularities $V_n = 2\Delta/en$

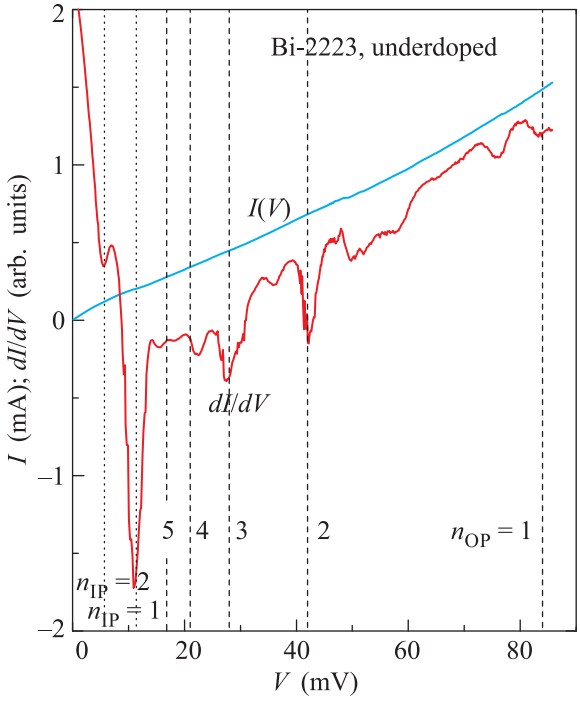

Fig. 7. $I(V)$- and dI/dV-curves for nanocontact in Andreev regime in underdoped Bi-2223 (sample TEO2, $T = 4.2$ K, $T_c = 104 \pm 5$ K, $\Delta_{OP} = 42 \pm 0.5$ meV, $\Delta_{IP} = 5.7 \pm 0.7$ meV, $2\Delta_{OP}/kT_c = 9.4 \pm 0.5$, $2\Delta_{IP}/kT_c = 1.3 \pm 0.3$). Vertical dashed lines correspond to expected positions of Andreev singularities $V_n = 2\Delta/en$

in cuprates there exists scaling of the gap Δ and T_c on doping. In underdoped cuprates reduction of a doping level p causes reduction of both Δ and T_c. For that reason we have assigned a smaller gap value to the internal CuO_2-plane (Tables 1–3). In [22] the assignment of the gaps was reversed without reliable grounds.

For cuprates the multigap scenario was first introduced by Kresin and Wolf ("chains-and-planes" model for $YBa_2Cu_3O_{7-x}$) [23]. The Kresin–Wolf theory was approved by several experimental studies [20, 24, 25]. Later a multigap scenario was applied to MgB_2 and iron-based superconductors – typical multiband systems [26]. The Leggett mode – a unique property of multigap superconductors [27] was detected in MgB_2 and $YBa_2Cu_3O_{7-x}$, demonstrating the importance of relative phase oscillations between different condensates [20, 28]. In the present investigation we deal with another class of multigap superconductors, where doping plays a decisive role.

5. Conclusion. In the present investigation Andreev and tunneling spectroscopy studies of $Bi_2Sr_2Ca_{n-1}Cu_nO_{2n+4+\delta}$, $HgBa_2Ca_{n-1}Cu_nO_{2n+2+\delta}$, and $Tl_2Ba_2Ca_{n-1}Cu_nO_{2n+4+\delta}$ have shown that superconductivity in single-layer and two-layer phases has a single-gap character. Qualitatively different results were obtained for three-layer phases. In doped Hg-1223, Bi-2223, and Tl-2223 samples two (or three) superconducting gaps were observed. The existence of multigap superconductivity in superconducting cuprates with $n \geq 3$ is explained by a difference in doping levels of outer (OP) and internal (IP) CuO_2-planes.

We take the opportunity to express sincere gratitude to V.M. Pudalov for useful discussions. This work was supported by RFBR (grants # 14-02-00700, 11-02-01201, 08-02-00935).

1. A. A. Abrikosov, Physica C **341–348**, 97 (2000); Physica C **317–318**, 154 (1999); preprint: cond-mat/9912394, 21 Dec (1999).
2. K. Gofron, J. C. Campuzano, A. A. Abrikosov, M. Lindroos, A. Bansil, H. Ding, D. Koelling, and B. Dabrowski, Phys. Rev. Lett. **73**, 3302 (1994).
3. C. Kendziora, R. J. Kelley, and M. Onellion, Phys. Rev. Lett. **77**, 727 (1996).

4. M. R. Presland, J. L. Tallon, R. G. Buckley, R. S. Liu, and N. E. Flower, Physica C **176**, 95 (1991).
5. Ya. G. Ponomarev, H. H. Van, S. A. Kuzmichev, S. V. Kulbachinskii, M. G. Mikheev, M. V. Sudakova, and S. N. Tchesnokov, JETP Lett. **96**, 743 (2012).
6. Ya. Ponomarev, M. Mikheev, M. Sudakova, S. Tchesnokov, and S. Kuzmichev, Phys. Stat. Sol. C **6**, 2072 (2009).
7. H. Mukuda, S. Shimizu, A. Iyoi, and Y. Kitaoka, J. Phys. Soc. Jpn. **81**, 011008 (2012).
8. X.-J. Chen, V. V. Struzhkin, Zh. Wu, R. J. Hemley, and H. Mao, Phys. Rev. B **75**, 134504 (2007).
9. V. A. Alyoshin, D. A. Mikhailova, E. B. Rudnyi, and E. V. Antipov. Physica C **383**, 59 (2002).
10. S. N. Putilin, E. V. Antipov, O. Chmaissem, and M. Marezio, Nature **362**, 226 (1993); S. N. Putilin, E. V. Antipov, and M. Marezio, Physica **212**, 266 (1993).
11. A. Krapf, G. Lacayo, G. Kastner et al., Supercond. Sci. Technol. **4**, 237 (1991).
12. T. E. Oskina, Ya. G. Ponomarev, H. Piel et al., Physica C: Superconductivity **266**, 115 (1996).
13. G. E. Blonder, M. Tinkham, and T. M. Klapwijk, Phys. Rev. B **25**, 4515 (1982); M. Octavio, M. Tinkham, G. E. Blonder, and T. M. Klapwijk, Phys. Rev. B **27**, 6739 (1983); K. Flensberg, J. B. Hansen, and M. Octavio, Phys. Rev. B **38**, 8707 (1988).
14. R. Kummel, U. Gunsenheimer, and R. Nicolsky, Phys. Rev. B **42**, 3992 (1990).
15. J. C. Cuevas, A. Martin-Rodero, and A. Levy Yeyati, Phys. Rev. B **54**, 7366 (1996); A. Poenicke, J. C. Cuevas, and M. Fogelström, Phys. Rev. B **65**, 220510R (2002).
16. T. P. Devereaux and P. Fulde, Phys. Rev. B **47**, 14638 (1993).
17. D. Daghero and R. S Gonnelli, Supercond. Sci. Technol. **23**, 043001 (2010).
18. E. S. Itskevich, V. F. Kraĭdenov, and I. G. Kuzemskaya, JETP **91**(3), 562 (2000).
19. B. Vignolle, D. Vignolles, D. LeBoeuf, S. Lepault, B. Ramshaw, R. Liang, D. A. Bonnb, W. N. Hardyb, N. Doiron-Leyraud, A. Carrington, N. E. Hussey, L. Taillefer, and C. Proust, C. R. Physique **12**, 446 (2011).
20. S. V. Kulbachinskii, Ya. G. Ponomarev, L. M. Fisher, and O. V. Belyaeva, JETP Lett. **96**, 35 (2012).
21. W. Guyard, M. Le Tacon, M. Cazayous, A. Sacuto, A. Georges, and D. Colson, arXiv:0708.3732v1 [cond-mat.supr-con] (2007).
22. N. Miyakawa, K. Tokiwa, T. Watanabe, A. Iyo, and Y. Tanaka, AIP Conf. Proc. **850**, 397 (2006).
23. V. Z. Kresin and S. Wolf, Phys. Rev. B **46**, 6458 (1992).
24. N. Klein, N. Tellmann, H. Schulz, K. Urban, S. A. Wolf, and V. Z. Kresin, Phys. Rev. Let. **71**, 3355 (1993).
25. B. A. Aminov, M. A. Hein, G. Müller et al., J. Supercond. **7**, 361 (1994).
26. H. J. Choi, D. Roundy, H. Sun et al., Nature **418**, 758 (2002).
27. A. J. Leggett, Prog. of Theor. Phys. **36**, 901 (1966).
28. Ya. G. Ponomarev, S. A. Kuzmichev, M. G. Mikheev et al., Sol. State Comm. **129**, 85 (2004).